

INTEGRATING FIELD AND REMOTE SENSING ANALYSES OF ABOVEGROUND
BIOMASS DYNAMICS DURING SECONDARY FOREST
REGENERATION IN COSTA RICA

by

KELSI LYN DAVIS

JASON C. SENKBEIL, COMMITTEE CHAIR
ANGÉLICA M. ALMEYDA ZAMBRANO
CHRISTINA L. STAUDHAMMER
MATTHEW C. LAFEVOR
EBEN N. BROADBENT

A THESIS

Submitted in partial fulfillment of the requirements
for the degree of Master of Science
in the Department of Geography
in the Graduate School of
The University of Alabama

TUSCALOOSA, ALABAMA

2017

Copyright Kelsi Lyn Davis 2017
ALL RIGHTS RESERVED

ABSTRACT

The process tropical aboveground biomass (AGB) plays in the global carbon cycle is imperative to preserve in the efforts to combat the effects of climate change through climate mitigation strategies. However, there is currently an insufficient understanding of AGB distribution and dynamics in tropical forests, and a lack of time and cost-effective means of estimating AGB. Species identification, location, diameter-at-breast-height (DBH), and AGB were determined at the stem-level in four 0.5 ha plots in a Costa Rican tropical wet forest to assess the distributional patterns of AGB, and its partitioning among various forest stand ages. Remotely-sensed data of the plots was collected utilizing a PrecisionHawk Rev4 unmanned aerial system (UAS) equipped with a dual-return light detection and ranging (LiDAR) sensor to calibrate with field data to determine if it could accurately estimate AGB in a densely forested environment.

Species richness varied among forest stand ages, and had a slight negative impact on AGB at a fine spatial scale. Tree stems 5 – 24 cm in DBH represent over 80% of all stems included in the AGB analyses, yet contribute less than half of the total AGB represented among the plots. Vegetation distribution and characteristics of biomass clustering evolved with forest stand age. Height metrics were extracted from a LiDAR-derived digital elevation model (DEM) and digital surface model (DSM), and predictive calibration models were generated to estimate AGB from the remotely-sensed data. However, extracting height metrics from the LiDAR data emphasized the challenges associated with accurate spatial modeling of a dense tropical forest

DEDICATION

I would like to dedicate this thesis to everyone who has supported me during my time at The University of Alabama. Specifically, I would like to dedicate this thesis to my committee members, my friends and family, and my husband Michael Schwind.

LIST OF ABBREVIATIONS AND SYMBOLS

AGB	Aboveground biomass
AGB_{est}	Estimated aboveground biomass for the biomass model
AGL	Above ground level
CHM	Canopy height map
DBH	Diameter at breast height
D	Diameter at breast height variable for the biomass model
DEM	Digital elevation model
DSM	Digital surface model
GIS	Geographic information system
GNSS	Global navigation satellite system
H	Height variable for the biomass model
IMU	Inertial measurement unit
LiDAR	Light detection and ranging
n	Sample size
p	Probability of the occurrence under the conditions of the null hypothesis as more or less extreme than the value observed
ρ	Wood density variable for the estimated biomass model
TCH	Top of canopy height
UAS	Unmanned aerial system
UTM	Universal Transverse Mercator coordinate system

WGS World Geodetic System

> Greater than

< Less than

\geq Greater than or equal to

\leq Less than or equal to

= Equal to

ACKNOWLEDGEMENTS

I am appreciative of the opportunity to recognize and thank everyone that has assisted me with my research and academic endeavors while attending The University of Alabama. First, I would like to thank Eben Broadbent and Angélica Almeyda Zambrano, who I am most indebted to for the opportunity to attend The University of Alabama and the ability to pursue research in tropical forestry. This study would not have been possible without their continuous inspiration, field and logistical support, expertise, and the innumerable funding and presentation opportunities they have provided to me. I would also like to thank Christina Staudhammer, for her valuable input and counsel during the process of completing my thesis. I am also indebted to Jason Senkbeil for his supportive advice, dependability, and agreeing to be my formal advisor and chairperson of my committee. I would also like to thank Matthew LaFevor for his participation as a committee member.

Receiving my Master's degree would not have been possible without the wonderful friends and family I am fortunate to have. I thank my loving family who have always encouraged me to pursue my goals and persist, even in the face of adversity. I especially want to thank my dad, whose love, guidance, and high expectations of me has always fostered the strong will necessary to achieve my goals. I would also like to thank my friends, especially those in the graduate program at The University of Alabama, for their moral support and the countless nights of laughter that made this journey so memorable.

Finally, I would like to thank Michael Schwind, my husband. Your unceasing love and support, even hundreds of miles away, has played such a critical role in where I am today. Thank you for your assistance during my field work and analyses, your words of kindness and encouragement, and your unreserved faith that I can do anything I put my mind to.

CONTENTS

ABSTRACT	ii
DEDICATION	iii
LIST OF ABBREVIATIONS AND SYMBOLS	iv
ACKNOWLEDGEMENTS	vi
LIST OF TABLES	x
LIST OF FIGURES	xi
1. INTRODUCTION	1
2. MATERIALS AND METHODS.....	5
2.1. Study area.....	5
2.2. Field biomass estimates	7
2.3. Species and structural diversity	8
2.4. Distribution of biomass.....	9
2.5. Remotely sensed data collection and estimates	1
3. RESULTS	12
3.1. Species and structural diversity	12
3.2. Vegetation distribution.....	15
3.3. Aboveground biomass clustering.....	15
3.4. Spatially derived biomass estimates	18

4. DISCUSSION.....	20
4.1. Species and structural characteristics and biomass.....	20
4.2. Forest vegetation and biomass distribution.....	21
4.3. Spatial data calibration.....	22
4.4. Research limitations.....	23
5. CONCLUSION.....	24
REFERENCES	26

LIST OF TABLES

1. General characteristics of the study plots	7
2. Species and structural composition.....	12
3. Analysis of variance results from the linear mixed-effect model	13
4. Proportion of total AGB in DBH classes	15

LIST OF FIGURES

1. The Osa Peninsula.....	6
2. Marginal Mean AGB	13
3. Stem proportions by DBH class.....	14
4. Vegetation and biomass distribution.....	17
5. LiDAR derived point cloud	19

1. INTRODUCTION

Tropical aboveground biomass (AGB) plays a critical role in the carbon cycle as an efficient carbon reservoir, sequestering approximately 40 to 50% of all vegetative terrestrial carbon, more atmospheric carbon than any other terrestrial ecosystem (Feldpaush *et al.*, 2012; Kindermann *et al.*, 2008; Lewis *et al.*, 2009). Tropical deforestation and degradation is reported to be the second greatest cause of global anthropogenic greenhouse emissions (IPCC 2007; Kindermann *et al.*, 2008), and estimated to generate approximately 25% of total human-induced carbon emissions (Kindermann *et al.*, 2008). Accumulation of forest biomass has the potential to serve as a significant carbon sink, and is now a substantial part of mitigation strategies to combat climate change (Dahlin *et al.*, 2012). However, there is large uncertainty as to the role of biomass in the carbon cycle because of its distributional variation across landscapes (Houghton, 2009; Saatchi *et al.*, 2007), uncertainty concerning deforestation, (Houghton, 2007), and limited reliable biomass data (Saatchi *et al.*, 2007; Houghton *et al.*, 2009; Alves *et al.*, 2010). To further incorporate AGB in climate change mitigation policy implementation, uncertainty associated with carbon storage of tropical biomass must be reduced. Accurate AGB estimates at local and regional levels are necessary to elucidate carbon stock dynamics (Broadbent *et al.*, 2008), to better determine the role of tropical deforestation in the carbon cycle, and to create more accurate scenario models (Urquiza-Haas *et al.*, 2007; Houghton *et al.*, 2009; Loarie *et al.*, 2009; Alves *et al.*, 2010). To accurately map carbon stocks, a greater understanding of spatial and compositional uncertainty associated with biomass partitioning, as well as better methods of efficient and

accurate biomass estimation, such as utilizing unmanned aerial system (UAS) technologies, must be explored.

Uncertainty in tropical forest AGB measurements arise due to the proliferation of tree species and sizes, as well as inter-specific variation in tree form. Species and structural diversity have also been linked to AGB and carbon stock (Ali *et al.*, 2016), and has been extensively explored since the 1990's (Dănescu *et al.*, 2016; Zhang *et al.*, 2012). Species and structural diversity characteristics and complexity of forest ecosystems depend largely on stand maturity and evolve as a forest ages (Lei *et al.*, 2009; Zhang and Chen, 2015; Ali *et al.*, 2016). Indeed, there is substantial support for the long-standing hypothesis that AGB increases with forest stand age. However, the relationship between species and structural diversity on AGB in tropical forests is insufficiently understood (Van Con *et al.*, 2013), and has been far less studied in forested environments (Vance-Chalcraft *et al.*, 2010; Van Con *et al.*, 2013) Previous studies have revealed that stand structural diversity has considerable influence on biomass and carbon storage in forested environments (e.g. Ali *et al.*, 2016). Despite generally positive species diversity and biomass relationships in forests, some studies have presented conflicting results, revealing negative or insignificant correlations (Van Con *et al.*, 2013). Thus, there is a need to further examine the complex relationships between AGB, structural diversity, and stand complexity in tropical forests. Additionally, uncertainty arises from variation in stand disturbance history, leading to different stand ages or variation in stand structure and composition, as well as different vegetative and AGB distribution patterns. In young tropical forests, previous literature has revealed that clustering of vegetation is common among young pioneer species (Seidler and Plotkin, 2006). However, there appears to be insufficient research performing geospatial analyses to assess clustering patterns of vegetation and AGB distribution in tropical forests among various

forest stand ages that may increase the accuracy of AGB inventories. Utilizing stem coordinates and a geographic information system (GIS) provides the ability to determine statistically significant distribution and clustering patterns, as well as assess their species and structural characteristics.

Efficient methods of biomass quantification that incorporate spatial and temporal variation must be developed and employed at global scales for climate mitigation strategies. It is also important to develop low-cost, timely, and accurate means of quantifying AGB estimates across broad landscapes and at the land-owner level (Zahawi *et al.*, 2015). Conventional field measurements are essential for localized AGB estimates (Asner *et al.*, 2012), but lack recognition of the variation in biomass and carbon storage across landscapes (Asner *et al.*, 2012; Goetz *et al.*, 2009). However, measurements of biomass at the field plot level can be labor intensive, costly, and difficult to update on shorter time intervals (Houghton, 2005). The potential for biomass estimation that provides more accurate quantification across landscapes lies in remote sensing technologies (Houghton and Goetz, 2008; Dubayah *et al.*, 2010). Light detection and ranging (LiDAR), a method that utilizes laser pulses capable of penetrating forest canopies, can enable measurements of structural forest attributes and can be calibrated with field data for biomass estimates at broader spatial scales (Asner *et al.*, 2012; Lefsky *et al.*, 2002). Research has revealed that LiDAR is the best choice for accurate and precise estimation of biomass (Hansen *et al.*, 2015; Fassnacht *et al.*, 2014; Zolkos *et al.* 2013). However, the price of conventional manned-aircraft methods for LiDAR data acquisition are generally at least \$20,000 USD regardless of study size, and often excludes the cost of data processing (Erdody and Moskal, 2010; Zahawi *et al.*, 2015). Recently, UAS platforms have provided a less expensive means of spatial data acquisition (Zahawi *et al.*, 2015; Anderson and Gaston, 2013). Accurate,

localized AGB estimates utilizing UAS platforms could provide a cost and time effective means of further understanding the role tropical forest biomass plays in the global carbon cycle, and prove useful for climate mitigation strategies.

This study seeks to examine the distributional patterns of AGB with respect to forest stand age, and species and structural diversity in regenerating secondary forests in southwestern Costa Rica and determine if UAS-based LiDAR is capable of accurately estimating biomass. Primary inquiries addressed in this study were: (1) What is the relationship between species-diversity and AGB? (2) What is the species and structural diversity associated with various regenerating successional forest stages? (3) What are the spatial distributional and clustering patterns of vegetation and biomass partitioning in various forest stand ages? (4) Can a UAS-based LiDAR be used in combination with field measurements to accurately estimate AGB across spatial variation and among various forest stand ages?

2. MATERIALS AND METHODS

2.1. Study area

This study was conducted in the Osa Peninsula, located in the southern-most region of the Pacific Coast of Costa Rica (Oviedo and Solís, 2008) (Figure 1). Spatial and field data collection took place in close proximity to the Piro Biological Station (8°24'14.6" N, 83°20'11.6" W), in a tropical wet forest environment (Life Zone map; Sanchez-Azofeifa *et al.* (2002). The Osa Peninsula is dominated by various evergreen tropical forests (Sanchez-Azofeifa *et al.*, 2002) and remains the largest lowland contiguous forest on the Pacific Central American coast (Gottfried *et al.*, 1994; Ankersen *et al.*, 2006). The Osa Peninsula encompasses remarkable levels of endemism and biodiversity, including the highest tree diversity in Central America, and has been called one of the world's most biologically intense locations (Ankersen *et al.*, 2006). Additionally, its canopy is higher than most Neotropical rainforests (Taylor *et al.*, 2015).

Substantial annual precipitation and consistently high temperatures contribute to the tropical landscape of the Osa Peninsula. Despite a pronounced drier season from January to March, the region receives over 5,000 mm of rainfall annually, with warm temperatures that average 26°C (Cleveland *et al.*, 2002). Nearly all the vegetation withstands the brief drier season and an evergreen landscape persists year-round (Tosi 1975; Cleveland *et al.*, 2002). Three seafloor volcanic events occurring during the Late Cretaceous and Early Tertiary period are responsible for the formation of the Osa Peninsula and its diverse geological features (Berrange and Thorpe 1988; Cleveland *et al.*, 2002).

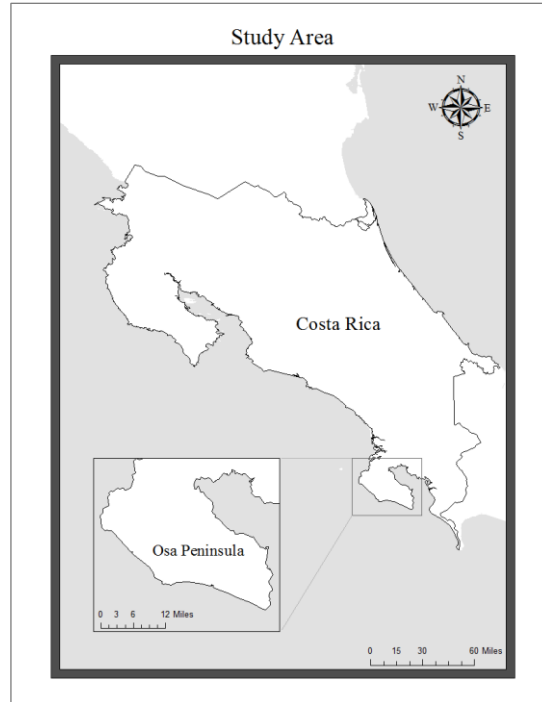


Fig. 1. The Osa Peninsula
Map portraying the study area where this research was conducted.

Segments of the region that were submerged in the sea more recently have created an array of bedrock ages and soil varieties (Berrange and Thorpe, 1988; Cleveland *et al.*, 2002). The peninsula is approximately 60 km in length (Sak *et al.*, 2004) and has an elevational range of 200 to 760 meters (Sanchez-Azofeifa *et al.*, 2002).

In this study, four 50 m x 100 m (0.5 ha) forested field plots established for previous studies (see Morales-Salazar *et al.*, 2012; Morales-Salazar *et al.*, 2013) were utilized. Each field plot encompassed fifty 10 m x 10 m contiguous subplots. All plots were located within 3.5 km of the Piro Biological Station. Three field plots represented various secondary forest successional stages following disturbance, and one plot served as a primary forest control with no recognized previous disturbance (Table 1).

Table 1.
General characteristics of the study plots

Study Plot	Forest Age (years)	Location	2016 AGB (kg)	Tree density (/0.5 ha)	Total species	Mean DBH (cm)
Youngest Secondary	13 - 23	8°23'48" N, 83°18'22" W	30,661	404	49	12.2
Intermediate	23 – 38	8°24'51" N, 83°20'57" W	58,083	353	49	15.0
Mature Secondary	> 38	8°24'01" N, 83°20'17" W	73,549	468	76	14.2
Primary	Primary	8°24'40" N, 83°20'22" W	157,915	394	100	16.4

2.2. Field biomass estimates

Baseline data was available from two previous studies conducted in 2009 and 2013, and consisted of diameter at breast height (DBH; cm), tree height (m) from visual and regional allometric estimates, wood density (g/m^3), and species identification. A diameter tape was used to determine the DBH (cm) at 1.3 m height above ground level (AGL) for all woody stems ≥ 5 cm DBH. DBH for irregular stems was measured at a height above the stem irregularity, as determined by previous researchers. Ground tapes were positioned at the subplot-level for each respective subplot origin to determine the Cartesian coordinates of every stem. Height and wood density were recorded for each incorporated woody stem because they have been identified as important predictive variables that improve AGB estimate models (Chave *et al.*, 2005).

Field data collection for this study took place from June to August, 2016. DBH and relative x-y subplot coordinates were collected. Additional woody stems that were not included in the previous data were incorporated if they met the minimum DBH threshold of 5 cm. Because of the limited time available for field work, stem height was estimated using a regional diameter-to-height model (Navarro *et al.*, 2013). For each tree individual that did not have baseline wood density data available, a local expert identified the species. The mean wood density (g/m^3) was found at the finest taxonomic value utilizing the Global Wood Density

Database (Chave *et al.*, 2009; Zanne *et al.*, 2009). AGB was estimated by applying the recommended best predictive model for wet forest stands following Chave *et al.* (2005):

$$AGB_{est} = 0.0776 \times (\rho D^2 H)^{0.940}$$

Where; AGB_{est} is the estimated AGB (kg), ρ is the wood density (g/m^3), D is DBH (cm), and H is height (m). Plot-level and subplot-level AGB estimates were determined by summing the AGB of encompassed stems.

2.3. Species and structural diversity

Species richness, commonly utilized in species diversity and productivity analyses (Vance-Chalcraft *et al.*, 2010; Martinez-Sanchez and Cabrales, 2012; Van Con *et al.*, 2013), was determined at both the plot-level and subplot-level scale to examine the relationship of species diversity and plot age on AGB. Rarefied species richness was determined at the plot-level utilizing the vegan package (Vegan: Community Ecology Package, Version 2.3-5) in program R version 3.3.3 (R Core Team, 2016). Subplot-level richness was determined as the number of species present in each subplot and excluded unidentified stems ($n = 15$).

Variograms were generated in R utilizing the gstat package (Gräler *et al.*, 2016) to visually assess potential spatial autocorrelation of AGB within each plot. The Incremental Spatial Autocorrelation and Global Moran's Spatial Autocorrelation tools were further applied to the plots in ArcMap 10.2.2 to determine if significant spatial autocorrelation was present for stem AGB at 95% confidence. A linear mixed-effect model was generated in R using the lmerTest package (Kuznetsova *et al.*, 2016) to assess AGB as a function of forest stand age, species richness, and their interaction at the stem level ($n = 1,825$) and excluded unidentified stems ($n = 15$). A random effect for each subplot was included in the model to address

correlation among trees within each subplot sampled. While a random effect for subplots within plots could account for correlation among subplots within the plot, autocorrelation analyses did not detect significant spatial autocorrelation within plots, and it was therefore excluded from the linear mixed-effect model. A Kenward-Rogers adjustment was used to estimate the degrees of freedom in type 3 tests of fixed effects. A natural log transformation was necessary to meet the assumptions of normality and homoscedasticity of the model residuals. Marginal (least square) means were generated to further illuminate significant model effects.

To further examine the relationship of stand structural diversity on AGB partitioning in this tropical lowland forest, stems were classified into eight discrete 10-cm classes of DBH. Discrete classes increased in DBH value by increments of 10 cm starting with 5 - 14.9 cm (Class 1), and the final class (Class 8) grouped all stems ≥ 75 cm. Partitioning of AGB by structural diversity was investigated by determining the total and proportion of biomass in each DBH class for the plots. DBH mean, minimum, and maximum values were determined for each plot (Table 2).

2.4. Distribution of biomass

Spatial analyses assessing the distribution of stems and AGB clustering in the field plots were completed using ArcMap 10.2.2 Spatial Statistics toolbox. X-Y Cartesian coordinate data were georeferenced and projected in WGS 1984 UTM Zone 17N to create the subsequent woody individuals and stem shapefiles. The Average Nearest Neighbor analysis was conducted for each plot to examine the distribution of woody vegetation of the successional forest ages. Multi-stemmed individuals were considered as one individual tree in the Nearest Neighbor analysis to avoid overrepresentation of a single specimen. To assess patterns of biomass distribution, the Hot Spot Analysis Tool was applied to each plot. AGB clustering was identified as significant

when the Hot Spot Analysis Getis-Ord G_i^* p-value was less than 0.05. All recorded stems were included in the Hot Spot Analysis to ensure appropriate biomass values and further examine the partitioning of biomass among stems and clusters defined as a set of points within 6 meters of neighboring stems. Trends of species diversity and structural attributes were assessed for each significant cluster of biomass to further reveal the patterns of biomass partitioning among the forest stand ages.

2.5. Remotely sensed data collection and estimates

Remotely sensed data were collected in June, 2016. A fixed-wing PrecisionHawk Rev4 UAS platform was equipped with a Velodyne VLP-16 dual-return LiDAR sensor, a tactical grade Novatel IMU and single-frequency GNSS, and employed for spatial data acquisition. The platform was flown at 100 meters AGL and 20 meters above the forest canopy. A Trimble Geo7x with a Zephyr 2 external antenna served as a base station and acquired data during the flights, and the data were post-processed to obtain ≤ 10 cm horizontal and vertical accuracy. LiDAR data from both flights for each study plot were merged using LASTools. A digital elevation model (DEM) and digital surface model (DSM) were produced from the point clouds in ENVI LiDAR at 50 cm spatial resolution. A procedure was developed in ArcGIS to interpolate the DEM using an inverse distance weighted algorithm because of low ground point density from the dense tropical vegetation. A canopy height map (CHM) for each plot was calculated at 50 cm resolution by subtracting the plot DEM from the plot DSM. Top-of-canopy height (TCH), mean, and minimum height metrics were extracted from the CHMs at 10 m x 10 m subplot resolution ($n = 199$) and excluded ground returns. Quantile range outliers were also excluded from further analyses ($n = 1$). Extracted height metrics were calibrated with field AGB estimates via a simple linear regression (Zahawi *et al.*, 2015) in JMP

(JMP®, Version 13.0) in order to parametrize predictive models. Spatial AGB estimates were determined using the predictive models and regressed against the field AGB estimates.

Predictive models were evaluated using the root mean square error (RMSE) and coefficient of determination (r^2).

3. RESULTS

3.1. Species and structural diversity

A total of 189 species were identified among the study plots. The primary control and mature secondary plots had the highest diversity, exhibiting a rarefied richness of 95 and 68 species, respectively (Table 2). The second youngest secondary plot had a rarefied richness of 49 species, and the youngest plot displayed less than half of the diversity of the primary with a richness of 47 species. The most abundant tree species differed by plot, and species dominance, in terms of the number of individuals of the most abundant species, was higher in the intermediate (*Guazuma ulmifolia*) and youngest secondary plots (*Inga thibaudiana*). Tree individuals of the species *Guazuma ulmifolia* contributed over half of the total AGB in the intermediate plot. Fewer individuals of a single species were present in the primary control (*Symphonia globulifera*) and mature secondary plot (*Lonchocarpus macrophyllus*), and did not contribute as considerably to the total AGB.

Table 2.
Species and structural composition

Variable	<i>Study plot</i>			
	Youngest secondary	Intermediate	Mature secondary	Primary
Rarefied richness	47	49	68	95
Most abundant species	<i>Inga thibaudiana</i>	<i>Guazuma ulmifolia</i>	<i>Lonchocarpus macrophyllus</i>	<i>Symphonia globulifera</i>
Species Density (individuals)	70	116	39	40
Abundant species proportion of total AGB (kg)	0.16	0.61	0.097	0.071
Mean DBH (cm)	12.2	15.0	14.2	16.4
Maximum DBH (cm)	48	61	83	203
DBH range (cm)	43	56	78	198

Variograms of the plots did not display noticeable trends of AGB spatial autocorrelation (results not shown). Furthermore, both the Incremental Spatial Autocorrelation and Global Moran’s Spatial Autocorrelation analyses indicated insignificant autocorrelation of AGB within the study plots ($p > 0.05$). Results of the linear mixed-effect model indicate that species richness significantly influenced AGB (Table 3). However, the effect of richness on AGB did not significantly differ by forest stand age, and stand age did not significantly influence AGB. Model results suggest that species richness has a slightly negative effect on AGB within each plot, when the effect of stand age was included in the model (Figure 2).

Table 3.
Analysis of variance results from the linear mixed-effect model

Variable	Mean square	Degrees of freedom	F. value	p - value
Age	4.7	717	2.09	0.100
Richness	18.7	425	8.22	0.004
Age*Richness	1.8	525	0.81	0.489

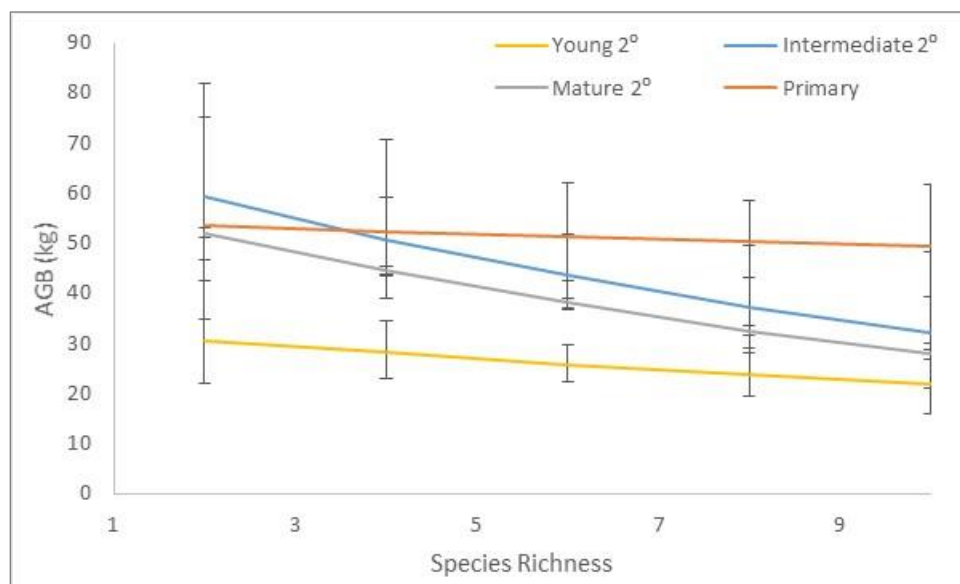


Fig. 2. Marginal mean AGB
Marginal mean values of AGB by forest type as richness increases.

The distribution of DBH values varied among the plots (Figure 3). The youngest secondary plot had the smallest mean DBH and the primary control had the largest mean DBH at over 4 cm greater. Interestingly, the intermediate plot had a higher mean DBH than the mature secondary despite its younger stand age. The range and maximum DBH values increased with forest age. Stems in DBH classes 1 and 2 (5 – 24 cm) were the most abundant, representing over 80% of total stems among all forest stand ages. These stems contributed a substantial proportion of the total biomass in the intermediate and youngest secondary plots, at 37% and 53% of the total AGB, respectively (Table 4). However, they represent a much smaller proportion of biomass in the mature secondary and primary plot, at 27% and 11%, respectively. Stems above 55 cm DBH constitute a small number of the total stems ($n = 19$), but represent an extraordinary proportion of total AGB among the plots (33%). Only six stems that were ≥ 75 cm DBH in the primary control plot accounted for nearly half the total AGB encompassed within the plot.

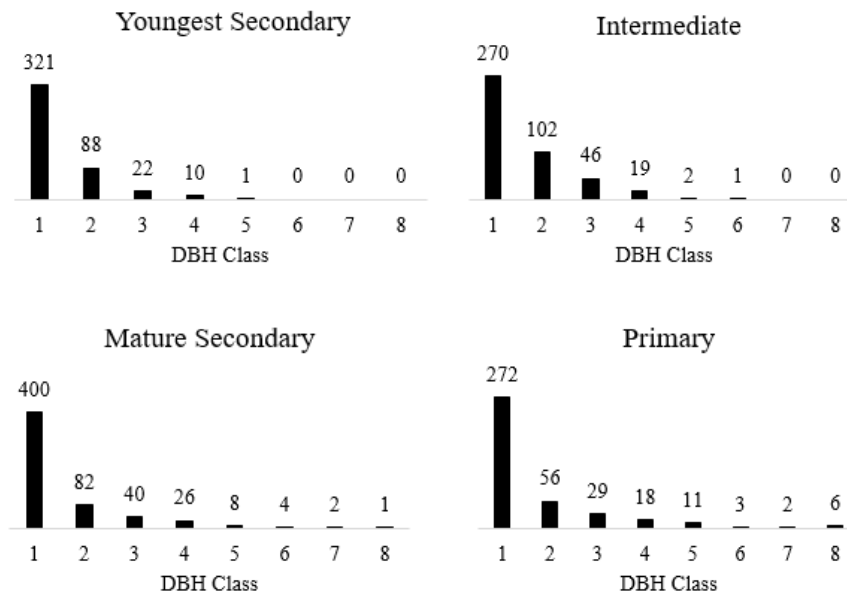


Fig. 3. Stem proportions by DBH class
Stem DBH structural diversity in the forested field plots

Table 4.
Proportion of total AGB in DBH classes

DBH class	<i>Study plot</i>			
	Youngest Secondary	Intermediate	Mature Secondary	Primary
1	0.18	0.12	0.12	0.04
2	0.35	0.25	0.15	0.07
3	0.24	0.32	0.19	0.10
4	0.20	0.24	0.26	0.10
5	0.03	0.03	0.12	0.12
6	0.00	0.04	0.07	0.04
7	0.00	0	0.05	0.04
8	0.00	0	0.04	0.50

3.2. Vegetation distribution

Results from the Average Nearest Neighbor Analysis indicated a change in woody vegetative spatial distribution trends as the forests matured. The intermediate and youngest secondary plots exhibited a significantly clustered tree distribution at ($p = 0.013$) and ($p = 0.003$), respectively, with the youngest plot displaying the strongest clustering trend. The mature secondary plot displayed a statistically random (non-clustered and non-dispersed) pattern of tree distribution. The primary control was not characterized by clustering of tree individuals, but rather displayed a statistically significant pattern of dispersed woody vegetation ($p = .0004$)

3.3. Aboveground biomass clustering

The Hot Spot Analysis identified 7 significant clusters in the youngest secondary plot, encompassing 8 species (Figure 4). Clusters 4, 5, and 6 each consisted of a single stem with a DBH greater than the plot mean (12.2 cm). The single-stems in clusters 4 and 6 represent less than 0.1% of the plot-total AGB. However, cluster 7 encompassed one of the largest stems present within the plot, and accounted for approximately 2.8% of the total AGB. Cluster 1 consisted of 5 stems and included the largest tree in the youngest secondary plot, accounting for over 3.8% of plot biomass. Clusters 2 and 3 each included a stem in DBH class 1, as well as a

larger stem in DBH class 3 or 4. Clusters 2 and 3 represented 3.2% and 2.3% of the biomass, respectively. 3 stems comprised cluster 3, which encompassed a large stem of 40.2 cm DBH and represented roughly 2% of the AGB.

The Hot Spot Analysis identified three significant clusters of AGB in the intermediate plot. The various clusters were comprised of 35 stems in total, and encompassed 13 species in total. All clusters enclosed tree individuals with multiple stems ≥ 5 cm that were included in field AGB estimates. This trend is most prevalent in cluster 3, which encompasses a single tree individual with 7 stems. The intermediate plot includes the individual with the maximum DBH and stem-level AGB within the plot, and cluster 2 is dominated by stems in DBH classes 2, 3, and 4. Clusters 1, 2, and 3 represent approximately 6.3%, 5.9%, and 9.7% of the plot-total AGB, respectively.

There were 6 significant clusters identified in the mature secondary plot and included a total of 13 species. Clusters 1, 3, 5 each encompassed a single stem that contributed less than 0.003% of the total AGB, and likely resulted in statistical significance of clustering because of their relatively isolated location. 75% of the stems in cluster 2 are in DBH class 4 and the cluster represents approximately 4.4% of the plot AGB. Cluster 4 consists of numerous stems, many belonging to a single individual and two trees in DBH class 4 and represents the highest proportion of the plot biomass exceeding 6.4%. Cluster 6 is comprised of three stems representing 5.4% of the total AGB. Two trees with 39 and 83 cm DBH values greatly contribute to the significance of this cluster.

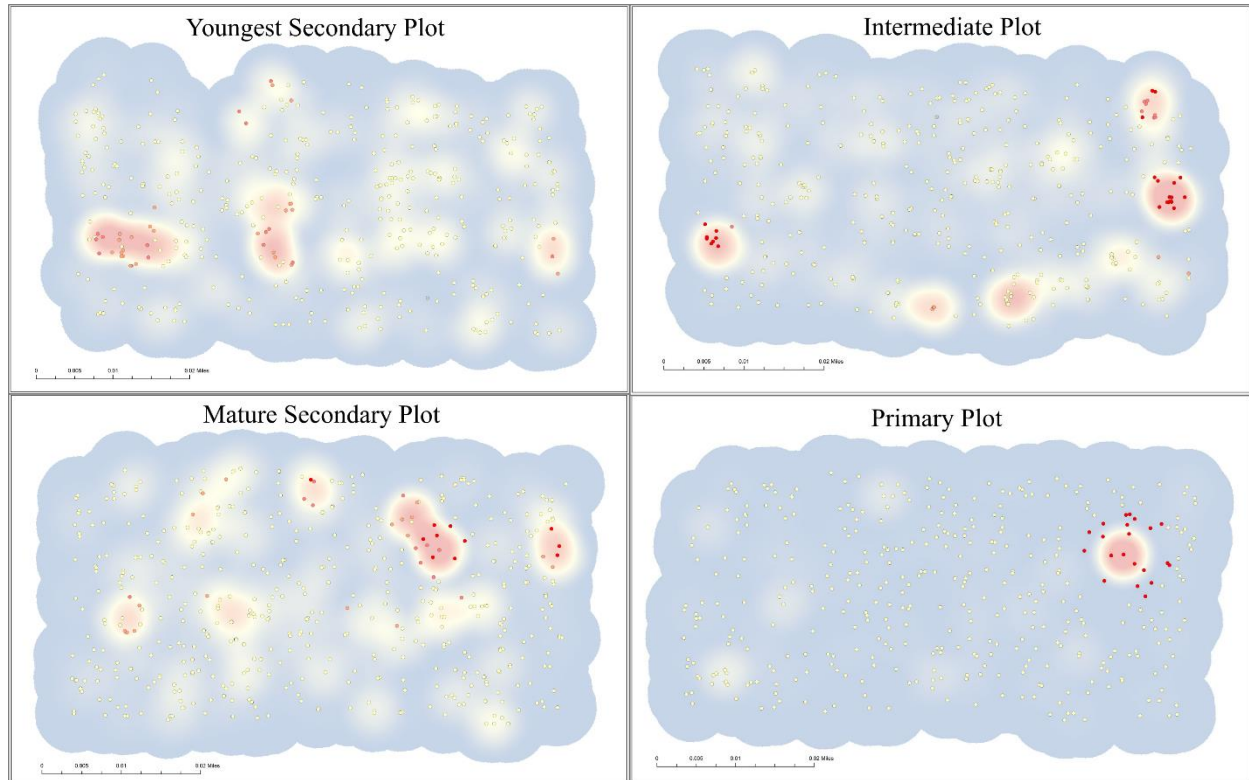


Fig. 4. Vegetation and biomass distribution

Maps of the study plots depicting the significant clusters of AGB and a heat density map displaying increasing quantities of AGB. Red represents significant clusters and increasing AGB quantities.

The Hot Spot Analysis identified a single cluster of AGB in the primary control plot. This cluster encompasses the stem with the maximum DBH in the plot, and remaining stems included have much lower DBH values and were likely included because of their proximity to the large individual. The cluster exhibits high diversity and encompasses 20 various species. No tree individuals have multiple identified stems. Approximately 27% of the total AGB of the primary plot is comprised by stems included within this cluster, and the large stem comprises 25% of this alone.

3.4. Spatially derived biomass estimates

The point clouds (Figure 5) derived from the LiDAR data resulted in sparse ground returns that were difficult to identify. Height extracted from the CHMs generated from the Velodyne VLP-15 dual-return LiDAR-generated DEM and DSM resulted in TCH data exceeding 97 m in the primary forest plot. These TCH values greatly surpass the maximum anticipated height of approximately 60 m in the primary forest and suggest that the generated CHM resulted in inaccurate TCH metrics. The inaccuracy of the CHMs can likely be attributed to the generation of the DEM by means of interpolation utilizing the inverse distance weighted algorithm with such sparse ground points and the inability to identify true ground returns. For the purposes of this study, the process of calibrating the CHM extracted height metric data to the field estimated AGB was still completed to test the methodological approach. Results of the field and spatial calibration regressions did not reveal strong correlations between the predictive models and the field AGB estimates. AGB predictive models still resulted in RMSE values over 550 m, and r^2 values ≤ 0.14 . However, the inaccuracy of the height metrics obtained from the CHMs to create the predictive models may have greatly contributed to the weak correlations and the calibration approach should be reassessed when height metrics can be extracted from a more accurate DEM.

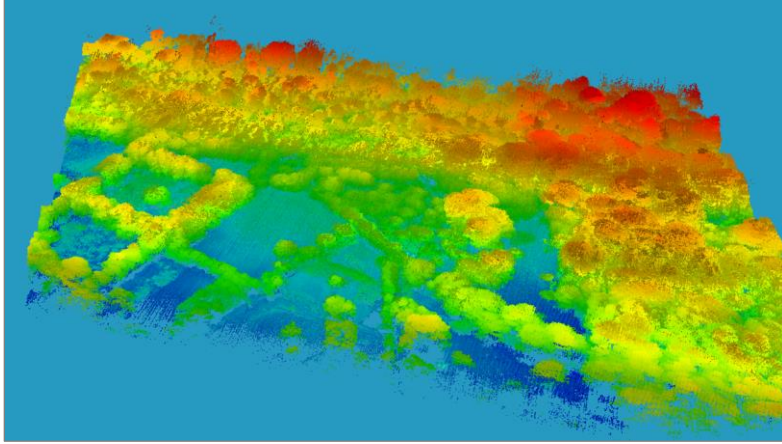


Fig. 5. LiDAR derived point cloud

Merged flight point cloud derived from the LiDAR data of the intermediate plot. This point cloud was utilized to generate the DEM and DSM for the intermediate plot.

4. DISCUSSION

It is critical to further understand AGB dynamics in tropical forests and to develop efficient methods of AGB estimation for climate mitigation strategies. Assessing the complex patterns of AGB distribution regarding species and structural characteristics may result in more accurate inventory estimates and improve spatial estimations of AGB in the future. Remote sensing technologies have emerged that are capable of estimating AGB in a timely manner, but little has been done to investigate the capabilities of time and cost-efficient UAS technologies to accurately quantify biomass. The results of this study sought to analyze AGB distribution in a dense tropical rainforest and to determine the capabilities of cost-efficient UAS technologies to estimate AGB.

4.1. Species and structural characteristics and biomass

The highest species richness was present in the primary control plot, and the youngest successional forest plot had the lowest rarefied diversity. Total AGB and plot-level rarefied species richness of the field plots increased with maturing stand age. Results of the linear mixed-effects model indicate that species richness slightly decreased AGB at a finer spatial scale, but this effect was significant given forest stand age was in the model. Moreover, marginal means show this effect was weak, and only present for intermediate and mature secondary forests. These results provide additional contradictory findings of the relationship between species richness and biomass, and further research should assess this relationship with greater sample sizes and at larger spatial scales. Over 80% of all stems in each of the plots were 5 -24 cm DBH,

yet contributed less than half of the total plot AGB with the exception of the youngest secondary plot. Most AGB was represented among far fewer stems in higher DBH classes, highlighting the importance of preserving old-growth stems to maintain carbon stocks. The mean DBH in the mature secondary plot was lower than the intermediate plot. This deviation from the expectation that the mature secondary plot would have a higher mean DBH indicates distinct environmental factors influencing tree growth and composition between the two plots. Variables that could be responsible for this anomaly and should be considered in future ecological studies assessing the plots include microclimate, edaphic characteristics, light availability, and topographic features. Specifically, further efforts could focus on the impact of a steep east-facing slope on the vegetation in the mature secondary plot, where mass failure appears to have eliminated vegetation and may hinder further growth.

4.2. Forest vegetation and biomass distribution

The distribution of vegetation evolved as forest stand age matured. The youngest secondary and intermediate forest plots had significantly clustered trees and the mature secondary plot had a random distribution. Trends of AGB clustering in the youngest secondary plot were attributed to the presence of a few, large single-stem trees that were likely spared in the previous land disturbance. These results indicate that much AGB can still be preserved during land-use-land-change if practices focus efforts on preserving large stems. The presence of large trees and individuals with numerous stems contributed to patterns of clustering in the intermediate and mature secondary plots. Clustering in the primary control plot encompassed a stem with 203 cm DBH and surrounding trees that represented 27% of the plot total AGB. The presence of statistically significant clusters among the plots suggests the importance of utilizing larger scales for remotely sensed and ecological analyses, to ensure AGB hotspots are

incorporated into analyses that may be overlooked at finer scales. Amazingly, the primary plot had over five times the total AGB of the youngest secondary plot, and represented more than double the total AGB of the mature secondary plot. These findings further emphasize the importance of conservational efforts prioritizing preserving old-growth forests because of their substantial AGB and efficiency as carbon stocks relative to recovering secondary forests.

4.3. Spatial data calibration

Although this study successfully displayed the ability of a UAS equipped with a LiDAR sensor to be operated in a tropical rainforest environment, the dense canopy concealed the forest floor and resulted in sparse LiDAR ground returns that were difficult to distinguish from canopy returns in the understory. This issue presented more difficulties in plots with high topographic variation than plots that were relatively flat. Interpolation methods utilized to generate a LiDAR-derived DEM from such limited ground returns to create CHMs did not result in the extraction of accurate height metrics because of the sparse returns and inability to distinguish true ground returns. The predictive models generated from the height metrics, although still calibrated with the field data for the purposes of this study, revealed that this method of spatially-derived height metrics were inappropriate for estimating AGB, yielding high RMSE and low r^2 values associated with predictive models. Despite an accurate DSM, alternative methods of creating a DEM with such sparse ground points must be developed to obtain reliable height metrics to again evaluate the potential of spatial data to estimate AGB using this platform and LiDAR sensor. Further research will assess the potential of developing a DEM utilizing high-resolution satellite imagery in conjunction with the LiDAR point cloud and derived DSM should be further explored to determine if greater CHM accuracy can be achieved and AGB estimated from remotely-sensed data. It is anticipated that UAS platforms will continue to become more cost and

payload efficient, and that LiDAR sensors for UAS platforms will eventually have greater returns. This study focused on testing emerging UAS and LiDAR platforms, and future studies should be conducted to continue assess the capabilities of additional emerging platforms and sensors to estimate AGB as they are developed.

4.4. Research limitations

This study did not consider variability of the environmental factors among the study plots that influence tree growth and species composition and further research efforts could pursue characterizing these factors, as well as the land-use-history of these plots. Field-estimates of AGB were calculated utilizing the recommended Chave (2005) allometric model, which incorporates tree height as a variable. Inherent uncertainty lies in AGB estimates utilizing allometric equations, and incorporating tree height derived from diameter-height models rather than directly observed increases the uncertainty of these estimates. Another limitation of this study is the small sample size, including just four study plots. Including more field plots, replicating forest successional ages, however were beyond the scope of this project because of time and financial restraints. Including a larger sample size in future efforts, with the aim of providing statistical replication, would increase the power, confidence, and reliability of results.

5. CONCLUSION

A greater understanding of AGB dynamics in tropical forest ecosystems and the capabilities of cost and time-effective remote sensing technologies to estimate AGB will assist in more accurate, localized, and numerous biomass inventories in the future. AGB inventory data will be necessary for the implementation of climate change mitigation strategies aiming to reduce greenhouse gas emissions through reductions in tropical forest deforestation and degradation.

In this study of a Costa Rican tropical wet forest, species richness played a significant role in influencing AGB. Over 80% of the stems present among the study sites were 5 – 24 cm in DBH, but only represented over 40% the total AGB in the youngest secondary forest. Rather, more mature plots encompassing larger stems of lower abundance had greater values of total AGB and should be prioritized for carbon mitigation approaches focusing on preserving tropical forests.

This study examined the capabilities of calibrating LiDAR spatial data acquired with a UAS and dual-return LiDAR sensor with field-estimated AGB, but determined that the dense tropical canopy prevented enough ground returns to interpolate a DEM accurately and estimate AGB utilizing this approach. Ongoing efforts will continue to strive to develop methods to create a DEM that will reduce the error in the CHMs for more accurate height metrics and remotely-sensed AGB estimates. The time and cost efficiencies associated with the ability to accurately estimate AGB utilizing UAS technologies will enable AGB inventories to be conducted more

frequently and at larger spatial scales.

REFERENCES

- Ali, A., Yan, E., Chen, H. Y., Chang, S. X., Zhao, Y., Yang, X., & Xu, M. (2016). Stand structural diversity rather than species diversity enhances aboveground carbon storage in secondary subtropical forests in Eastern China. *Biogeosciences*, *13*(16), 4627.
- Alves, L. F., Vieira, S. A., Scaranello, M. A., Camargo, P. B., Santos, F. A., Joly, C. A., & Martinelli, L. A. (2010). Forest structure and live aboveground biomass variation along an elevational gradient of tropical Atlantic moist forest (Brazil). *Forest Ecology and Management*, *260*(5), 679-691.
- Anderson, K., & Gaston, K. J. (2013). Lightweight unmanned aerial vehicles will revolutionize spatial ecology. *Frontiers in Ecology and the Environment*, *11*(3), 138-146.
- Ankersen, T. T., Regan, K. E., & Mack, S. A. (2006). Towards a bioregional approach to tropical forest conservation: Costa Rica's Greater Osa Bioregion. *Futures*, *38*(4), 406-431.
- Asner, G. P., Clark, J. K., Mascaró, J., Vaudry, R., Chadwick, K. D., Vieilledent, G., ... & Knapp, D. E. (2012). Human and environmental controls over aboveground carbon storage in Madagascar. *Carbon balance and management*, *7*(1), 2.
- Asner, G. P., Mascaró, J., Muller-Landau, H. C., Vieilledent, G., Vaudry, R., Rasamoelina, M., ... & Van Breugel, M. (2012). A universal airborne LiDAR approach for tropical forest carbon mapping. *Oecologia*, *168*(4), 1147-1160.
- Berrangé, J. P., & Thorpe, R. S. (1988). The geology, geochemistry and emplacement of the Cretaceous-Tertiary ophiolitic Nicoya Complex of the Osa Peninsula, southern Costa Rica. *Tectonophysics*, *147*(3-4), 193-203.
- Broadbent, E. N., Asner, G. P., Peña-Claros, M., Palace, M., & Soriano, M. (2008). Spatial partitioning of biomass and diversity in a lowland Bolivian forest: Linking field and remote sensing measurements. *Forest Ecology and Management*, *255*(7), 2602-2616.
- Chave, J., Andalo, C., Brown, S., Cairns, M. A., Chambers, J. Q., Eamus, D., ... & Yamakura, T. (2005). Tree allometry and improved estimation of carbon stocks and balance in tropical forests. *Oecologia*, *145*(1), 87-99.
- Chave, J., Coomes, D., Jansen, S., Lewis, S. L., Swenson, N. G., & Zanne, A. E. (2009). Towards a worldwide wood economics spectrum. *Ecology letters*, *12*(4), 351-366.

- Cleveland, C. C., Townsend, A. R., & Schmidt, S. K. (2002). Phosphorus limitation of microbial processes in moist tropical forests: evidence from short-term laboratory incubations and field studies. *Ecosystems*, 5(7), 0680-0691.
- Dahlin, K. M., Asner, G. P., & Field, C. B. (2012). Environmental filtering and land-use history drive patterns in biomass accumulation in a mediterranean-type landscape. *Ecological Applications*, 22(1), 104-118.
- Dănescu, A., Albrecht, A. T., & Bauhus, J. (2016). Structural diversity promotes productivity of mixed, uneven-aged forests in southwestern Germany. *Oecologia*, 182(2), 319-333.
- Dubayah, R. O., Sheldon, S. L., Clark, D. B., Hofton, M. A., Blair, J. B., Hurtt, G. C., & Chazdon, R. L. (2010). Estimation of tropical forest height and biomass dynamics using lidar remote sensing at La Selva, Costa Rica. *Journal of Geophysical Research: Biogeosciences*, 115(G2).
- Erdody, T. L., & Moskal, L. M. (2010). Fusion of LiDAR and imagery for estimating forest canopy fuels. *Remote Sensing of Environment*, 114(4), 725-737.
- Fassnacht, F. E., Hartig, F., Latifi, H., Berger, C., Hernández, J., Corvalán, P., & Koch, B. (2014). Importance of sample size, data type and prediction method for remote sensing-based estimations of aboveground forest biomass. *Remote Sensing of Environment*, 154, 102-114.
- Feldpausch, T. R., Lloyd, J., Lewis, S. L., Brien, R. J., Gloor, M., Monteagudo Mendoza, A., ... & Phillips, O. L. (2012). Tree height integrated into pantropical forest biomass estimates. *Biogeosciences*, 3381-3403.
- Goetz, S. J., Baccini, A., Laporte, N. T., Johns, T., Walker, W., Kellndorfer, J., ... & Sun, M. (2009). Mapping and monitoring carbon stocks with satellite observations: a comparison of methods. *Carbon balance and management*, 4(1), 2.
- Gottfried, R. R., Brockett, C. D., & Davis, W. C. (1994). Models of sustainable development and forest resource management in Costa Rica. *Ecological Economics*, 9(2), 107-120.
- Gräler, B., Pebesma, E., & Heuvelink, G. (2016). Spatio-temporal interpolation using gstat. *R Journal*, 8(1), 204-218.
- Hansen, E. H., Gobakken, T., Bollandsås, O. M., Zahabu, E., & Næsset, E. (2015). Modeling aboveground biomass in dense tropical submontane rainforest using airborne laser scanner data. *Remote Sensing*, 7(1), 788-807.
- Houghton, R. A. (2005). Aboveground forest biomass and the global carbon balance. *Global Change Biology*, 11(6), 945-958.

- Houghton, R. A. (2007). Balancing the global carbon budget. *Annu. Rev. Earth Planet. Sci.*, 35, 313-347.
- Houghton, R. A., & Goetz, S. J. (2008). New satellites help quantify carbon sources and sinks. *Eos*, 89(43), 417-418.
- Houghton, R. A., Hall, F., & Goetz, S. J. (2009). Importance of biomass in the global carbon cycle. *Journal of Geophysical Research: Biogeosciences*, 114(G2).
- Intergovernmental Panel on Climate Change. (2007). Synthesis Report: Contribution of Working Groups I, II and III to the Fourth Assessment Report of the Intergovernmental Panel on Climate Change.
- Kindermann, G., Obersteiner, M., Sohngen, B., Sathaye, J., Andrasko, K., Rametsteiner, E., ... & Beach, R. (2008). Global cost estimates of reducing carbon emissions through avoided deforestation. *Proceedings of the National Academy of Sciences*, 105(30), 10302-10307.
- Kuznetsova, A., Brockhoff, P. B., Christensen, R. (2016) lmerTest: Tests in Linear Mixed Effects Models. R package version 2.0-33.
- Lefsky, M. A., Cohen, W. B., Parker, G. G., & Harding, D. J. (2002). Lidar remote sensing for ecosystem studies. *Bioscience*, 52(1), 19-30.
- Lei, X., Wang, W., & Peng, C. (2009). Relationships between stand growth and structural diversity in spruce-dominated forests in New Brunswick, Canada. *Canadian Journal of Forest Research*, 39(10), 1835-1847.
- Lewis, S. L., Lopez-Gonzalez, G., Sonké, B., Affum-Baffoe, K., Baker, T. R., Ojo, L. O., ... & Ewango, C. E. (2009). Increasing carbon storage in intact African tropical forests. *Nature*, 457(7232), 1003-1006.
- Loarie, S. R., Asner, G. P., & Field, C. B. (2009). Boosted carbon emissions from Amazon deforestation. *Geophysical Research Letters*, 36(14).
- Marvin, D. C., Asner, G. P., Knapp, D. E., Anderson, C. B., Martin, R. E., Sinca, F., & Tupayachi, R. (2014). Amazonian landscapes and the bias in field studies of forest structure and biomass. *Proceedings of the National Academy of Sciences*, 111(48), 5224-5232.
- Martinez-Sanchez, J. L., & Cabrales, L. C. (2012). Is there a relationship between floristic diversity and carbon stocks in tropical vegetation in Mexico?. *African Journal of Agricultural Research*, 7(17), 2584-2591.

- Morales-Salazar, M. S., Vílchez-Alvarado, B., Chazdon, R. L., Ortega-Gutiérrez, M., Ortiz-Malavassi, E., Guevara-Bonilla, M. (2012). Diversidad y estructura horizontal en los bosques tropicales del Corredor Biológico de Osa, Costa Rica. *Revista Forestal Mesoamericana Kurú*, 9(23), 19–28.
- Morales-Salazar, M. S., Vílchez-Alvarado, B., Chazdon, R. L., Ortiz-Malavasi, E., Guevara-Bonilla, M. (2013). Estructura, composición y diversidad vegetal en bosques tropicales del Corredor Biológico Osa, Costa Rica. *Revista Forestal Mesoamericana Kurú*, 10(24), 1–13.
- Navarro, M., Moya, R., Chazdon, R., Ortiz, E., & Vilchez, B. (2013). Successional variation in carbon content and wood specific gravity of four tropical tree species. *Bosque*, 34(1), 33-43.
- Oksanen, J., Blanchet, G. F., Friendly, M., Kindt, R., Legendre, P., McGlinn, D., ... & Wagner, H. (2017). *vegan: Community Ecology Package*. R package version 2.4-3. <https://CRAN.R-project.org/package=vegan>.
- Oviedo, L., & Solís, M. (2008). Underwater topography determines critical breeding habitat for humpback whales near Osa Peninsula, Costa Rica: implications for Marine Protected Areas. *Revista de Biología Tropical*, 56(2), 591-602.
- Saatchi, S. S., Houghton, R. A., Dos Santos Alvala, R. C., Soares, J. V., & Yu, Y. (2007). Distribution of aboveground live biomass in the Amazon basin. *Global Change Biology*, 13(4), 816-837.
- Sak, P. B., Fisher, D. M., & Gardner, T. W. (2004). Effects of subducting seafloor roughness on upper plate vertical tectonism: Osa Peninsula, Costa Rica. *Tectonics*, 23(1).
- Sanchez-Azofeifa, G. A., Rivard, B., Calvo, J., & Moorthy, I. (2002). Dynamics of tropical deforestation around national parks: remote sensing of forest change on the Osa Peninsula of Costa Rica. *Mountain Research and Development*, 22(4), 352-358.
- Seidler, T. G., & Plotkin, J. B. (2006). Seed dispersal and spatial pattern in tropical trees. *PLoS Biol*, 4(11), e344.
- Taylor, P., Asner, G., Dahlin, K., Anderson, C., Knapp, D., Martin, R., ... & Hofhansl, F. (2015). Landscape-scale controls on aboveground forest carbon stocks on the Osa Peninsula, Costa Rica. *PloS one*, 10(6), e0126748.
- Tosi, J. A. (1975). The Corcovado basin on the Osa Peninsula. *San José: Tropical Science Center*.
- Urquiza-Haas, T., Dolman, P. M., & Peres, C. A. (2007). Regional scale variation in forest structure and biomass in the Yucatan Peninsula, Mexico: effects of forest disturbance. *Forest Ecology and Management*, 247(1), 80-90.

- Vance-Chalcraft, H. D., Willig, M. R., Cox, S. B., Lugo, A. E., & Scatena, F. N. (2010). Relationship between aboveground biomass and multiple measures of biodiversity in subtropical forest of Puerto Rico. *Biotropica*, 42(3), 290-299.
- Van Con, T., Thang, N. T., Khiem, C. C., Quy, T. H., Lam, V. T., Van Do, T., & Sato, T. (2013). Relationship between aboveground biomass and measures of structure and species diversity in tropical forests of Vietnam. *Forest Ecology and management*, 310, 213-218.
- Zahawi, R. A., Dandois, J. P., Holl, K. D., Nadwodny, D., Reid, J. L., & Ellis, E. C. (2015). Using lightweight unmanned aerial vehicles to monitor tropical forest recovery. *Biological Conservation*, 186, 287-295.
- Zanne, A. E., Lopez-Gonzalez, G., Coomes, D. A., Ilic, J., Jansen, S., Lewis, S. L., Miller, R. B., Swenson, N. G., Wiemann, M. C., & Chave, J. (2009). Data from: towards a worldwide wood economics spectrum.
- Zhang, Y., & Chen, H. Y. (2015). Individual size inequality links forest diversity and above-ground biomass. *Journal of Ecology*, 103(5), 1245-1252.
- Zhang, Y., Chen, H. Y., & Reich, P. B. (2012). Forest productivity increases with evenness, species richness and trait variation: a global meta-analysis. *Journal of ecology*, 100(3), 742-749.
- Zolkos, S. G., Goetz, S. J., & Dubayah, R. (2013). A meta-analysis of terrestrial aboveground biomass estimation using lidar remote sensing. *Remote Sensing of Environment*, 128, 289-298.